Thermal Decomposition of Natural Fibers: Global Kinetic Modeling with Nonisothermal Thermogravimetric Analysis

Fei Yao,[1] Qinglin Wu,[1] Dingguo Zhou[2]

[1]*School of Renewable Natural Resources, Louisiana State University Agricultural Center, Baton Rouge, Louisiana 70803*
[2]*College of Wood Science and Technology, Nanjing Forestry University, Nanjing 210037, Jiangsu, China*

Received 24 January 2009; accepted 19 March 2009
DOI 10.1002/app.30439
Published online 15 June 2009 in Wiley InterScience (www.interscience.wiley.com).

ABSTRACT: The modeling of thermal decomposition process of ten natural fibers commonly used in polymer composite industry was performed by assuming a global model occurring within the entire degradation range with consideration of fiber as one pseudocomponent. Málek method with activation energy values previously obtained was applied to the modeling process. Careful calculation and evaluation indicated that, within an acceptable error limit of 5%, RO($n > 1$) model can be used to describe the degradation process of most selected fibers well. The other kinetic parameters used include activation energy range of 160–170 kJ/mol; parameter n in RO($n > 1$) = $(1 - \alpha)^n$ of 3–4; and ln A between 35 and 42 ln s^{-1}. Some condition limitations of the obtained model were also discussed. The model has practical significance in predicting fiber weight loss when the fiber is used in combination with engineering thermoplastics. © 2009 Wiley Periodicals, Inc. J Appl Polym Sci 114: 834–842, 2009

Key words: thermogravimetric analysis (TGA); composites; kinetics (polym.); modeling; fibers

INTRODUCTION

Natural fiber fillers from agricultural residues and forest products processing are subjected to thermal degradation during polymer composite processing. It is, therefore, of practical significance to understand and model the decomposition process of the fibers. Numerous kinetic schemes and models regarding to the fiber degradation process have been established.[1,2] However, it will be of more practical relevance to establish simplified kinetic models of the degradation of reinforcing fibers for polymer/natural fiber composite.

In our previous study,[3] thermal decomposition process and activation energy values of ten common natural fibers were investigated. It was found that thermal decomposition process of the selected natural fibers had similar thermogravimetric (TG) and differential thermogravimetric (DTG) curves as a result of being lignincellulosic material. The common thermal decomposition curves of fibers showed a distinct DTG peak (cellulose) and high-temperature "tails" (lignin). Also, the low-temperature "shoulder" can be seen in some fiber decomposition curves. The characteristics of all selected natural fibers showed that main thermal decomposition fraction (around 60%) happened in a temperature range of around 100°C (i.e., 215–310 ± 10°C in terms of extrapolated temperatures) for most natural fibers. The calculation result from isoconversional methods showed a stable apparent activation energy range of 160–170 kJ/mol for the most of selected fiber throughout the polymer processing temperature range. The objective of the study described in this article was to develop the practical modeling technique based on global kinetic scheme for the thermal degradation process of the fibers. In particular, the model and related kinetic parameters were developed by using a method demonstrated by Málek and coworkers.[4–6] Reaction mechanism and parameters of thermal decomposition process of natural fibers were described in detail.

THEORETICAL APPROACH

The kinetics of solid-state process is generally complicated.[6–8] A method proposed by Málek and

Correspondence to: Q. Wu (wuqing@lsu.edu).
Contract grant sponsor: USDA Rural Development Biomass Initiative Program; contract grant number: 68-3A75-6-508.
Contract grant sponsor: Louisiana Board of Regents Industrial Tie Subprogram; contract grant number: LEQSF: 2005-08-RD-B-01.

coworkers allows fairly reliable kinetic analysis and interpretation of nonisothermal TG-DTG data. This method has been described thoroughly in the cited literature.[4,6] A brief outline is shown below for consistence. Readers can refer to the original articles for details.

The fundamental expressions of analytical methods to calculate thermal decomposition kinetic parameters based on nonisothermal thermogravimetric analyzer (TGA) studies are generally described as

$$\frac{d\alpha}{dT} = \left(\frac{A}{\beta}\right) e^{-x} f(\alpha) \tag{1}$$

where T, A, β, and x are absolute temperature (K), pre-exponential factor (s^{-1}), heating rate (°C/min), and reduced apparent activation energy ($x = E_a/RT$), respectively. E_a and R are apparent activation energy (kJ/mol) and gas constant (8.314 J/K·mol), respectively. The conversion rate α has following expression:

$$\alpha = (W_0 - W_t)/(W_0 - W_f) \tag{2}$$

where W_t, W_0, and W_f are the sample weights at t, initial and final time, respectively. Function $f(\alpha)$ is an analytical expression describing the kinetic model of a reaction, which depends on the actual reaction mechanism. The most frequently used $f(\alpha)$ functions with their symbols are summarized in Table I.

By integration of eq. (1) in nonisothermal conditions, the following equation is obtained:

$$g(\alpha) = \int_0^\alpha \frac{1}{f(\alpha)} d\alpha = \int_0^T \frac{A}{\beta} e^{-x} dT = Ae^{-x}\left[\frac{T}{\beta}\pi(x)\right] \tag{3}$$

where $\pi(x)$ is an approximation of the temperature integral, which has the following sufficiently accurate approximation.[5]

$$\pi(x) = \frac{x^3 + 18x^2 + 88x + 96}{x^4 + 20x^3 + 120x^2 + 240x + 120} \tag{4}$$

Two new functions, $y(\alpha)$ and $z(\alpha)$, were then defined as below:

$$y(\alpha) = \left(\frac{d\alpha}{dt}\right) e^x = Af(\alpha) \tag{5}$$

$$z(\alpha) = \left(\frac{d\alpha}{dt}\right)\left[\pi(x)\frac{T}{\beta}\right] = f(\alpha)g(\alpha) \approx \left(\frac{d\alpha}{dt}\right) T^2 \tag{6}$$

One can easily transform experimental data to the $y(\alpha)$ and $z(\alpha)$ functions and then normalize them within the (0, 1) interval. Obviously, this can be done without the knowledge of any kinetic parameter in nonisothermal conditions. Two important parameters α_M and α_p^∞, at which the functions $y(\alpha)$ and $z(\alpha)$ have a maximum, respectively, are normally calculated by mathematical software. Then the function $f(\alpha)$ is determined through the schematic diagram introduced by Málek and coworkers.[4,6]

TABLE I
A Summary of Basic Thermal Kinetic Models

Models	Symbol	$f(\alpha)$
Johnson-Mehl-Avrami	JMA (n)	$n(1-\alpha)[-\ln(1-\alpha)]^{1-1/n}$
Reaction order law	RO (n)	$(1-\alpha)^n$
Autocatalytic (Šesták-Berggren)	SB (m,n)	$(1-\alpha)^n\,\alpha^m$
2D-diffusion	D2	$-1/\ln(1-\alpha)$
Jander equation	D3	$3(1-\alpha)^{(2/3)}/2[1-(1-\alpha)^{(1/3)}]$
Ginstling-Brounshtein	D4	$3/2[(1-\alpha)^{(-1/3)} - 1]$
Prout-Tompkins	PT	$\alpha\,(1-\alpha)$

As discussed in literatures, the apparent activation energy E_a is vital for the determination of function $y(\alpha)$.[4] Several recommended "model-free" methods (isoconversional methods) are presented in our previous article to calculate the decomposition activation energy values of selected fibers.[3] Those E_a values were then used to calculate function $y(\alpha)$ and $z(\alpha)$ in this study. The experimental data, α, T and $d\alpha/dt$, were obtained from TG-DTG curves directly.

EXPERIMENTAL

Ten natural fibers including wood, bamboo, agricultural residue, and bast fibers were used in this study. All raw materials were washed with water to remove the impurity and then dried in an oven at 75°C for 12 h. Dried materials were then ground with a Wiley mill, and then screened. The samples with the particle size between 20 and 28 meshes (0.9–1.3 mm) were collected for test.

Thermal decomposition was observed in terms of global mass loss by using a TA Instrument Q50 TGA. The samples were evenly and loosely distributed in an open sample pan with an initial sample amount of 8–10 mg. The temperature change was controlled from room temperature (25 ± 3°C) to 800°C at six different heating rates of 2, 3.5, 5, 7.5, 10, and 15°C/min in nitrogen atmosphere. The thermal decomposition was carried out at low or moderate heating rates to keep possible heat/mass-transfer intrusions at a minimum. The TG and DTG curves obtained were carefully smoothed and analyzed by using Universal Analysis 2000 software from TA Instruments. Relative parameters were calculated with a specially designed program in MS Excel or MATLAB software. Further details of experimental procedure were described elsewhere.[3]

RESULTS AND DISCUSSION

Determination of kinetics model and parameters

The thermogravimetric curves of 10 selected fibers in nonisothermal conditions were shown in our previous article along with the activation energy values. The E_a value of most fibers was quite stable (ca. 3%) in a conversion range of 0.1–0.6 according to three isoconversional methods. Thus, the activation energy values obtained can be used to calculate $y(\alpha)$ and $z(\alpha)$ functions. As shown in Table II, they were determined by averaging values from three isoconversional methods presented in the previous article.

The dependence of $y(\alpha)$ and $z(\alpha)$ functions on conversion rate α for various fibers is shown in Figure 1, using bagasse, kenaf, rice husk, and maple fibers as examples. Obviously, each individual $y(\alpha)$ function is concave and has a clear maximum α_M at $\alpha = 0$. The $y(\alpha)$ function curves of the other six fibers, which are not plotted here, also present similar concave shapes and α_M positions. Figure 1 also shows that various $z(\alpha)$ curves from degradation process of a certain fiber are close to each other. Each $z(\alpha)$ curve also exhibits a clear maximum, which is consistent with the fact that $z(\alpha)$ function has a maximum at α_p^∞ for all kinetic models summarized in Table I.[6] MATLAB software was then carefully operated to fit each single $[z(\alpha) - \alpha]$ curve to obtain the accurate values of α_p^∞.

TABLE II
The Values of Parameters α_M, α_p, and α_p^∞ Obtained from Corresponding $y(\alpha)$ and $z(\alpha)$ Function for 10 Fibers

Fiber	α_M	α_p	α_p^∞
Bagasse	0	0.67 (0.01)	0.69 (0.01)
Bamboo	0	0.57 (0.02)	0.59 (0.02)
Cotton stalk	0	0.61 (0.02)	0.62 (0.02)
Hemp	0	0.51 (0.01)	0.52 (0.01)
Jute	0	0.59 (0.02)	0.60 (0.02)
Kenaf	0	0.55 (0.01)	0.56 (0.02)
Rice husk	0	0.60 (0.01)	0.61 (0.00)
Rice straw	0	0.53 (0.02)	0.54 (0.02)
Wood-maple	0	0.69 (0.00)	0.70 (0.01)
Wood-pine	0	0.69 (0.01)	0.70 (0.01)

All critical values of $y(\alpha)$ and $z(\alpha)$ functions are summarized in Table II. It is clearly shown from α_M values (i.e., zero) and $y(\alpha)$ function shape (i.e., concave), as well as α_p^∞ values that the thermal

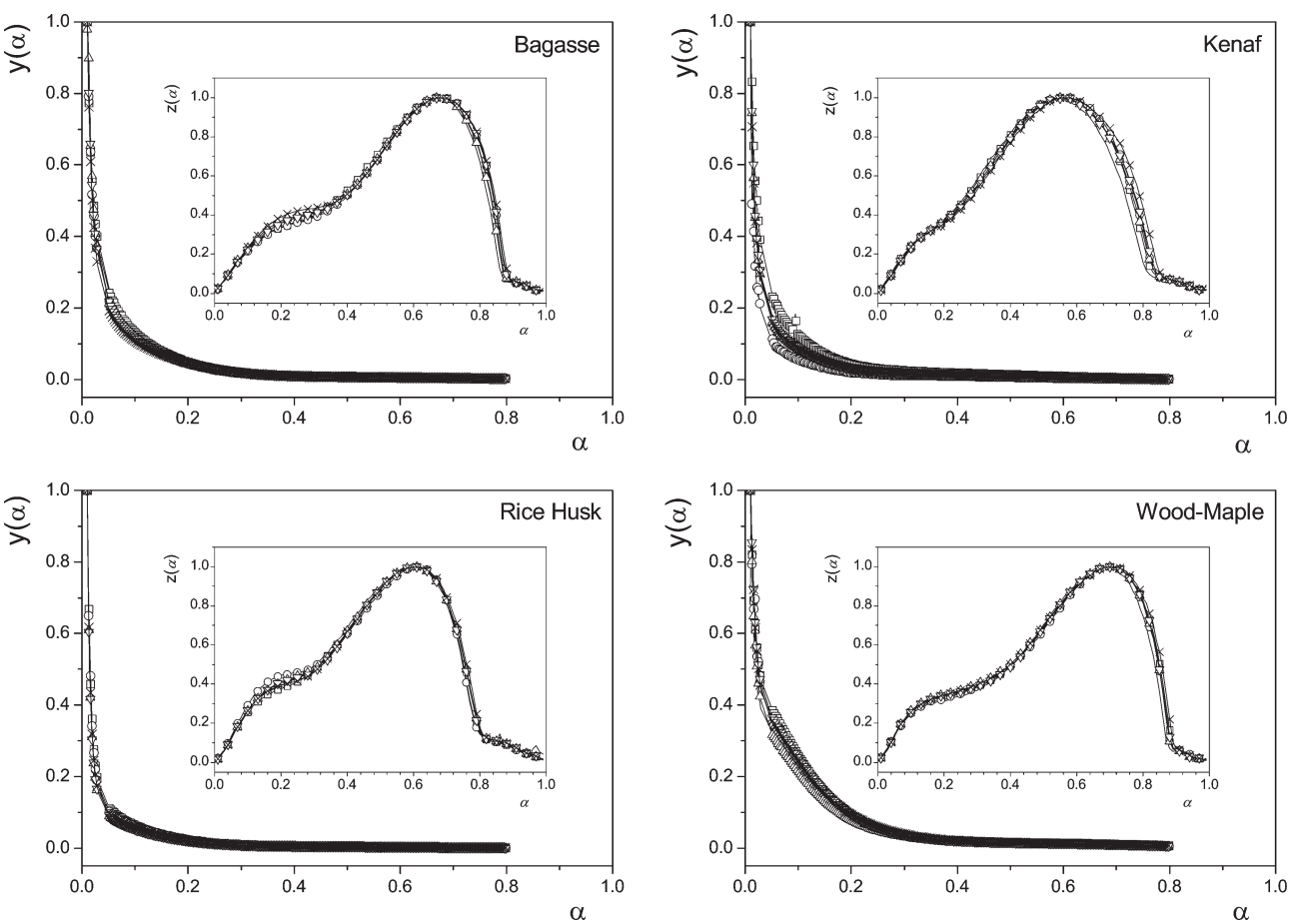

Figure 1 Normalized $y(\alpha)$ and $z(\alpha)$ functions corresponding to fiber thermal decomposition kinetic data using bagasse, kenaf, rice husk, and maple fibers as examples. The heating rates are shown in following symbols: 2°C/min (solid line); 3.5°C/min (-□-); 5°C/min (-○-); 7.5°C/min (-Δ-); 10°C/min (-▽-); and 15°C/min (-×-).

TABLE III
The Kinetic Parameters Obtained by Nonlinear Regression of Nonisothermal Data

Fiber	E (kJ/mol)	n	ln A (ln s^{-1})	fit (%)
Bagasse	168.6 (6.3)	3.25 (0.11)	38.14 (0.08)	4.67 (0.08)
Bamboo	160.9 (3.2)	3.85 (0.07)	37.45 (0.23)	3.57 (0.04)
Cotton stalk	171.8 (4.2)	3.77 (0.05)	39.15 (0.07)	4.32 (0.13)
Hemp	178.6 (6.6)	3.18 (0.26)	40.57 (0.12)	3.73 (0.18)
Jute	183.3 (9.0)	3.75 (0.26)	42.17 (0.10)	5.00 (0.02)
Kenaf	169.9 (2.1)	3.23 (0.17)	38.76 (0.07)	3.60 (0.07)
Rice husk	165.4 (2.9)	4.03 (0.19)	37.78 (0.10)	3.64 (0.07)
Wood-maple	153.3 (4.8)	3.04 (0.08)	34.47 (0.10)	4.79 (0.05)
Wood-pine	159.6 (3.9)	3.14 (0.08)	35.65 (0.05)	4.35 (0.18)
Rice straw	195.5 (2.5)	5.81 (0.17)	46.57 (0.12)	3.46 (0.09)
Average I[a]	167.9 (9.4)	3.47 (0.37)	38.24 (2.34)	4.19 (0.56)
Average II[b]	172.2 (1.3.5)	3.70 (0.82)	39.07 (3.44)	4.11 (0.59)

[a] Exclusive of values from rice straw fiber samples.
[b] Including values from rice straw fiber samples.

degradation kinetic model of fibers can be described using RO($n > 1$) model. With the knowledge of kinetic model, the equation for nonisothermal $\alpha(T)$ curve can be predicted from eq. (3) as

$$\alpha(T) = 1 - \left[1 - T\left(\frac{\pi(x)}{\beta}\right)(1-n)Ae^{-x}\right]^{1/(1-n)} \quad (7)$$

here, the $f(\alpha) = (1 - \alpha)^n$ for RO($n > 1$) model is used, and consequently,

$$g(\alpha) = \int_0^{\alpha} \frac{1}{f(\alpha)} d\alpha = \frac{1-(1-\alpha)^{1-n}}{1-n} \quad (8)$$

The temperature dependence of the reduced activation energy ($x = E_a/RT$) can be calculated from the average value of apparent activation energy obtained by isoconversional analysis. The key kinetic parameters A and n can be obtained by non-linear regression of experimental data using MATLAB software because each part of an entire kinetic equation is clearly defined. The average values of the parameter are summarized in Table III along with standard deviations, which were calculated from six different heating rates for each fiber type.

Comparison of experimental data (symbols) and predicted $\alpha(T)$ (lines) is shown in Figure 2 using bamboo, kenaf, rice straw, and pine fibers as examples. These $\alpha(T)$ curves were calculated using eq. (7) for the kinetic parameters shown in Table III. The other six fibers, which are not shown here, have similar results. There is good agreement between experimental data and prediction curves even though some discrepancies are observed at both very low and very high temperature (or, α) ranges. Those discrepancies were caused by the variability of activation energy and the strong dependence of the Málek method on activation energy values. However, one can expect a reasonable model if a good global agreement in the entire reaction process is reached. Therefore, the model obtained must be evaluated to quantify the goodness of fit (GOF). Moreover, latent force fitting caused by kinetic compensation effect (KCE) should also be evaluated.[9,10]

Evaluation of the kinetic parameters

The GOF of model is evaluated by the method of least squares (LSQ). The sum S of squared error of all picked points is defined as

$$S = \sum_1^N (y_i^{\text{obs}} - y_i^{\text{calc}})^2 \quad (9)$$

where y^{obs} is the experimental data and y^{calc} is the corresponding point of the calculated functions, subscript i indicates the discrete values of a given y, and the parameter N is the number of the data used in the curve fitting. The fitness between the observed and calculated values at the obtained parameters is given in percentage of the highest observed y value, $y_{\text{max}}^{\text{obs}}$:

$$\text{fit}(\%) = 100\frac{\sqrt{S/N}}{y_{\text{max}}^{\text{obs}}} \quad (10)$$

The method actually tests the error between observed and calculated values. Therefore, the output fit (%) is also referred as deviation (%) in some literatures.[11] The fitted result is shown in Table III. The good agreement, indicated by values <5%, was observed for all fibers. As shown in parentheses, the very small standard deviation of each fiber indicates the invariant GOF at different heating rates. Therefore, the error of the entire fitting was expected to be as low as 5%.

GOF is necessary, but not sufficient, for the evaluation of a thermal model, because it cannot evaluate

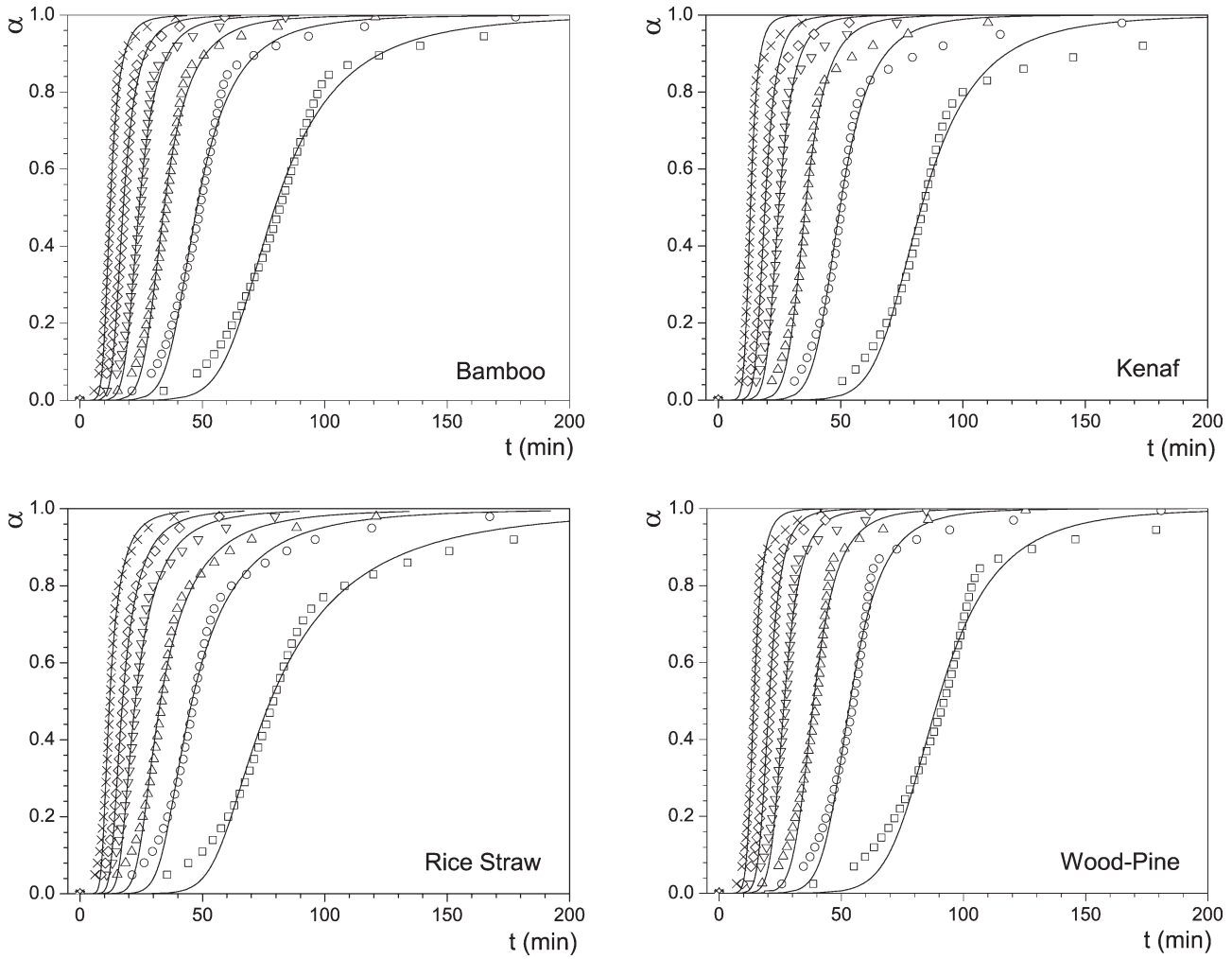

Figure 2 Nonisothermal TG curves for select fibers measured at different heating rates: 2°C/min (□); 3.5°C/min (○); 5°C/min (Δ); 7.5°C/min (▽); 10°C/min (◇) 15°C/min (×). Solid lines were calculated using eq. (7) for the kinetic parameters shown in Table III.

latent force fitting caused by KCE. KCE is caused by the exponent format of Arrehnius equation and refers to the fact that the covariability of parameter E and A makes experimental data possibly fit several different models well with different $f(\alpha)$.[12–14] It was reported that one might obtain extreme perfect fitting using F1 model on artificially produced A3 model curves.[15] An approach proposed by Perez-Maqueda etc.[15] helps offer an evaluation in this situation.

In this technique, through algebraic transformation, any function $f(\alpha)$ can be simplified from the empirical Šesták-Berggren equation as

$$f(\alpha) = c(1-\alpha)^n\alpha^m \tag{11}$$

using three constants c, n, and m. A logarithm transformation of eq. (1) (inserting $\beta = dT/dt$) leads to the following equation for fitting experimental data:

$$\ln\left(\frac{d\alpha/dt}{f(\alpha)}\right) = \ln cA - \frac{E_a}{RT} \tag{12}$$

Plotting the left hand side of eq. (12) with respect to the reciprocal of corresponding temperature, one can get a single straight line with slope $(-E_a/R)$ and the intercept (ln cA) if an appropriate function $f(\alpha)$ is chosen. It is worth noting that the key to this evaluation is to get a single straight line even using data from different heating rates. It was pointed out in the literature[15] that sometimes an inappropriate model can also lead to perfect straight lines, but those lines are parallel to each other instead of superposing on to one single curve.

Using this method, the linear relationship between $\ln[(d\alpha/dt)/f(\alpha)]$ and $1/T$ is plotted in Figure 3 after inserting obtained $f(\alpha)$ functions and experimental $d\alpha/dt$ and $1/T$ data into eq. (12) using bamboo, kenaf, rice husk, and maple fibers as examples. As

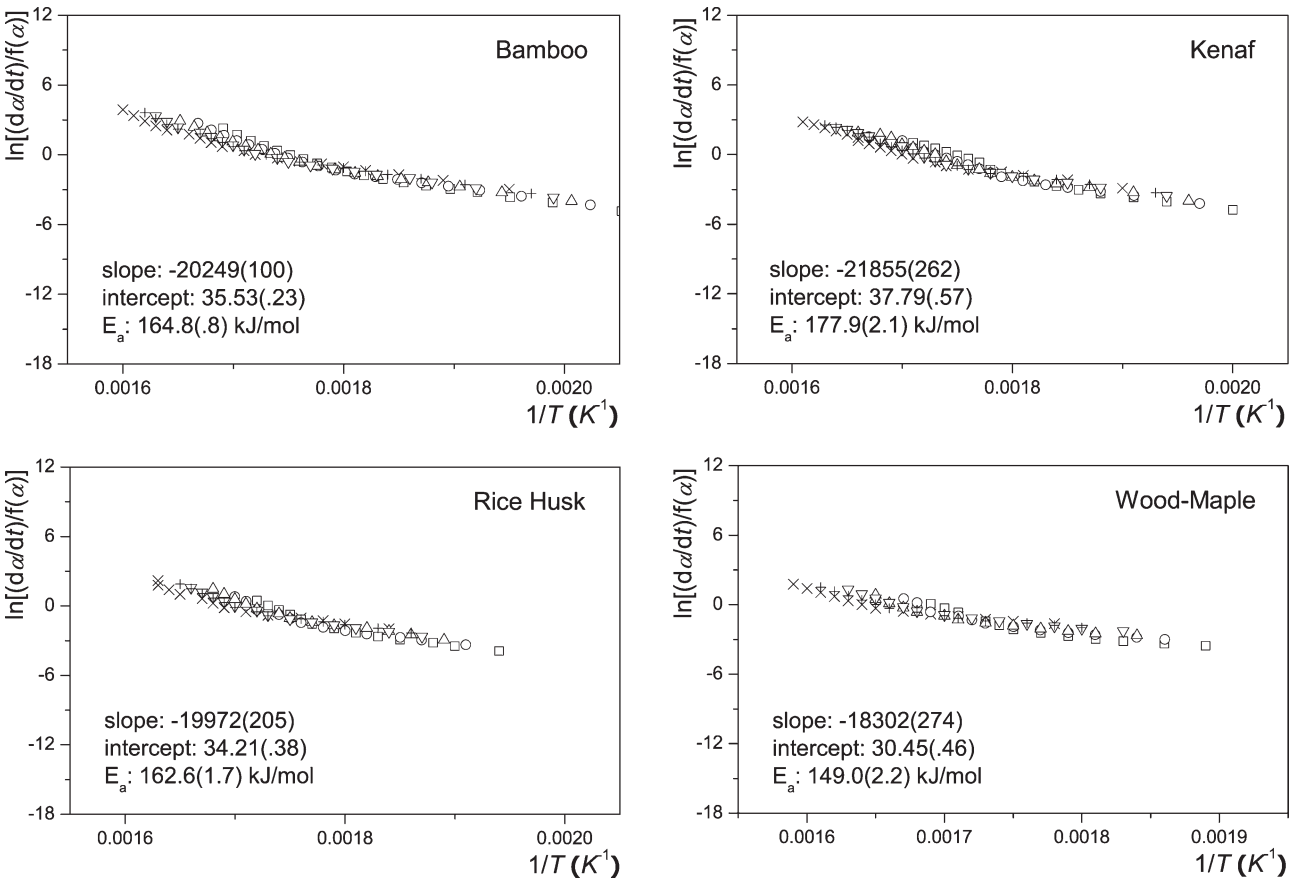

Figure 3 Single linear relationship between $[\ln(d\alpha/dt) - \ln f(\alpha)]$ and $1/T$ for four illustrational fibers at six heating rates: 2°C/min (□); 3.5°C/min (○); 5°C/min (Δ); 7.5°C/min (▽); 10°C/min (+); 15°C/min (×). The value before parenthesis is the average value of six slopes or intercepts whereas the value in parenthesis refers to standard deviation.

shown in the figure, for each fiber sample, six symbol lines corresponding to data from six different heating rates are overlapped with each other and yield a single straight line. The expression listed in each individual plot shows detailed slope and intercept. Here, the value before parenthesis is the average value of six slopes or intercepts while the value in parenthesis refers to standard deviation. Obviously, the superposition of six scatter lines is shown by a fairly small standard deviation (within 3% in most cases). The activation energy values listed in plots are calculated from the slope. They are quite comparable (error $< 2\%$) to those shown in Table III except that in the cases of jute (not plotted) and kenaf fibers the error reaches around 5%. In conclusion, the evaluation performed above shows that the model and relevant parameters obtained are appropriate for describing the degradation process of natural fibers.

Comparison of kinetic parameters of different fibers

On the basis of the calculated parameters shown in Table III, one can see a general trend of the degradation model for nine fibers (exclusive of rice straw fiber, which is obviously different with the others). Their degradation process has an activation energy range of 160–170 kJ/mol with an average of 168 kJ/mol, $f(\alpha)$ follows $\mathrm{RO}(n) = (1 - \alpha)^n$ model, parameter n has a range of 3–4 with an average of 3.5, and ln A is between 35 and 42 ln s^{-1} with an average of 38 ln s^{-1}.

Those intervals are fairly narrow ones, which may indicate the similarity of natural fiber degradation process. This observation was first mentioned in our previous article, where a narrow range of activation energy for most of the natural fibers was seen. As the energy barrier, the activation energy itself may provide the information of the critical energy needed to start a reaction. It implies the "difficulty" of starting a reaction. The similar activation energy values of various fibers indicated that critical energy of the decomposition reaction is similar among those fibers. However, only activation energy itself cannot be used to determine the "rate" of a reaction. Once a reaction starts, the question toward how fast the reaction is should be answered by the conversion function $f(\alpha)$ along with its parameters and pre-exponential factor A. Similar to the case of activation

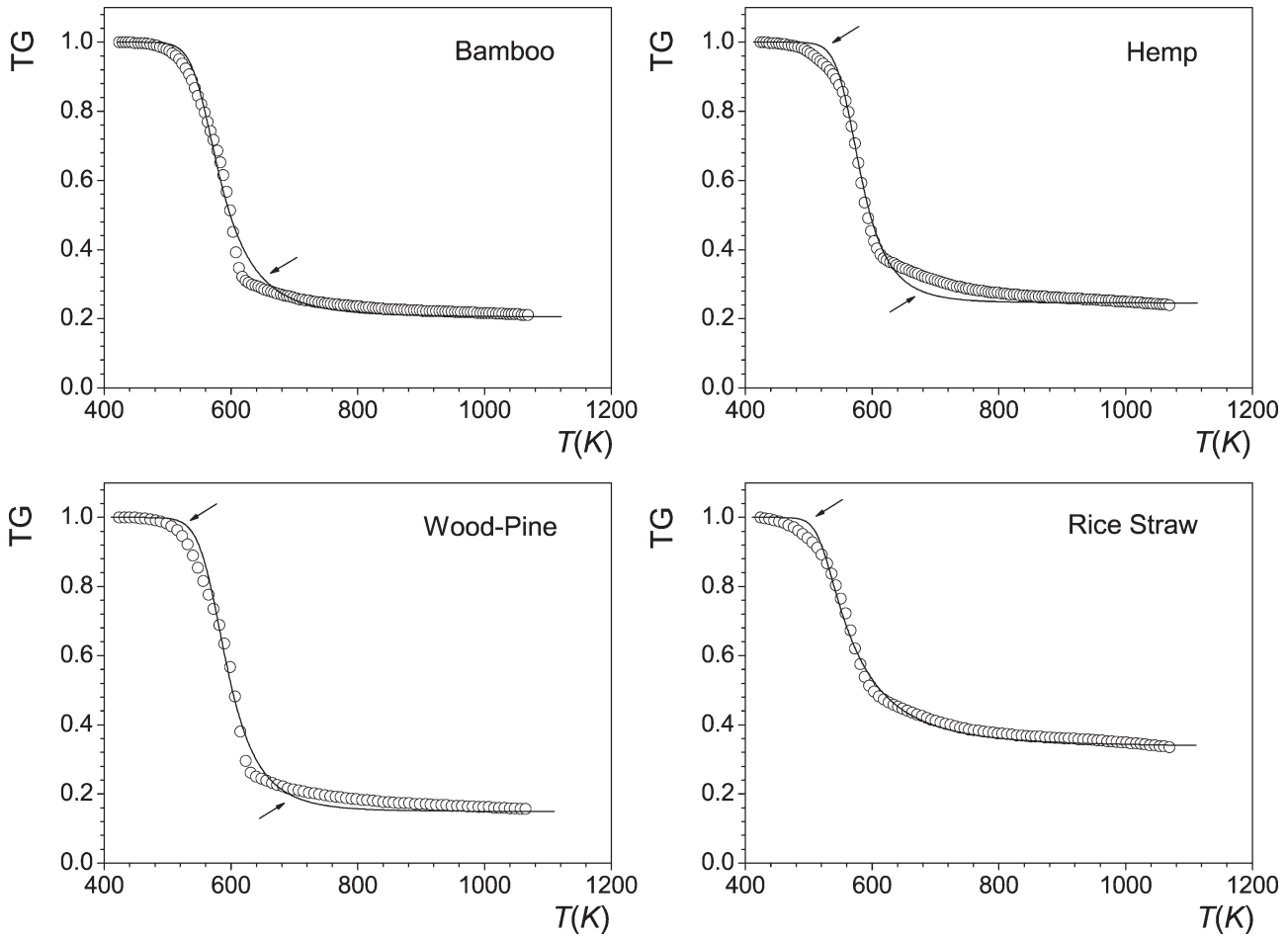

Figure 4 The comparison of predictive and experimental TG curves using four fibers as examples. Circle: experimental data; solid line: predicted curve. Arrows in the plots indicated the discrepancies.

energy, the closeness in parameters n or A among various fibers indicates a similar degradation rate of these fibers. The similarity of both "difficulty" and "rate" of fiber degradation reaction is associated with the similar elementary reactions of main components (cellulose, hemicelluloses, and lignin) of fibers. Unfortunately, such elementary reaction is very complex and is still ambiguous so far. The predictive mass fractions can be written as

$$\text{mass fraction}(\%) = 100\%[1 - \alpha(T)(1 - \text{residue})] \quad (13)$$

The predictive mass fractions vs. temperatures curve is also the predictive TG curve. By inserting the residues shown in our previous article, Figure 4 is plotted to validate the obtained predictive TG curves using bamboo, hemp, pine, and rice straw fibers degradation data at a heating rate of 5°C/min as examples. Also, a good agreement is obtained. Therefore, the kinetic model obtained is valid for predicting mass fractions of fibers with respect to temperature during thermal degradation.

The degradation processes of various fibers can be modeled with close parameters, but TG curves of those fibers are obviously different with each other.[3] It can be attributed to the different degradation residues of fibers. The residue is usually described as the first, tar or char generated during the degradation of fiber main components[1,16] and the second, degradation products of minor components in fiber composition. However, it is still ambiguous that when and how tar or char generate.[17,18] Also, it is still hard to clearly define the composition and structure of minor components of fibers (e.g., silicon in rice straw surface). However, degradation residues of a certain fiber are usually invariant under similar heating rates.[3] Its amount helps provide satisfied prediction in terms of global kinetics.

Discussions on modeling error, interpretation, and limitation

As mentioned, Málek method depends on accurate activation energy value E. Therefore, applying the average value E_a within α of 0.2–0.8 (or 0.3–0.7) rather than the entire range is strongly recommended because most reactions, especially solid-state ones,

are not stable at the beginning and ending periods. Different from a solution reaction, a solid-state reaction usually contains a diffusion process, the well-known mass and heat-transfer phenomenon[19,20] at the beginning period. It generates temperature and partial pressure gradient. Consequently, it generates reaction gradient from the outer to the inner surface of the solid sample. As a result, real activation energy values at this period are different from the ones at the middle period (0.1 or 0.2 to around 0.8). Thus, using apparent activation energy E_a to calculate the model parameters in this period will result in some discrepancies. In our case, the real conversion rates are correspondingly higher than model prediction shown in Figure 2. About the ending period, the long tail was observed in most DTG curves of fiber degradation, which is normally interpreted by lignin decomposition process characterized by the long-term and low activation energy. The reactant that exists here does not likely include cellulose and hemicelluloses any more. Consequently, activation energy level changed sharply. Similar to the situation in the beginning period, using apparent activation energy E_a to model the decomposition process in this period will also cause some discrepancies. In our case, the real conversion rates are correspondingly lower than model prediction as indicated in Figure 2. The fitting error obtained in this study is mostly caused by the mismatch in two periods mentioned earlier. Despite some discrepancies, the Málek method is still recommended for global thermal degradation modeling of natural fiber due to providing fairly reasonable process and acceptable error limits. This method makes it possible to obtain the kinetic triplets step by step instead of simultaneously whereas the latter might cause KCE. It has also been successfully applied in several fields, and in both nonisothermal and isothermal conditions.[21,22]

The obtained reaction model, RO($n > 1$), can be used to describe the degradation process of natural fibers with acceptable error limit. That is, weight losses of natural fibers can be estimated conveniently and rapidly in practical application of natural fiber filled polymer composites. However, it is necessary to avoid misleading readers in simply interpreting the mechanism of fiber degradation as a reaction order law. This is because the real degradation process of fiber was simplified to one reaction in this study due to the global model assumption. If a more complicated model (e.g., involving parallel, consecutive or competitive reactions, and more components) was assumed, the thermal degradation process of natural fiber will be interpreted in a different way. However, the complicated models may cause the difficulty in practical application. Also, some intensive researches are strongly expected on linking the interpretation of those involved reactions with physical and chemical process of real elementary reactions during fiber degradation. Therefore, the reaction order law obtained under global model assumption is still a possible choice from a macroscopical and practical perspective. This is also indicated by good fitting between experimental and simulative results not only from this study but also from some other researches applying the first order model to cellulose degradation.[1,8]

It was known that various experimental conditions (e.g., heating profile, heating rate, atmosphere, sample loading, and sample size and shape[23]) will affect modeling results of fiber degradation process. Therefore, the kinetic models obtained have the following limitations: medium fiber loading of 20–28 mesh irregular samples under comparatively low linear heating rates (i.e., 2–15°C/min) within a temperature range of 423–1073 K in nitrogen atmosphere for 10 selected natural fibers. Any change of conditions might cause a relevant change in the final result, e.g., more round particles instead of irregular fibers will cause corresponding excursion of DTG peak.[15] However, above conditions simulated practical utilization conditions of fiber for polymer composite, i.e., suitable fiber type and sample size (as used usually in composites), comparative sample loading (simulate the dispersion of fiber in feeding process), and, reasonable temperature range (show overall view and cover polymer processing temperature). Therefore, the model obtained still has practical significance in developing the technology for introducing natural fiber to engineering thermoplastic.

CONCLUSIONS

The modeling of thermal decomposition process of 10 natural fibers commonly used in polymer composite industry was performed by assuming a global model occurring within the entire degradation range with consideration of fiber as one pseudocomponent. Málek method with activation energy values previously obtained was applied to the modeling process. Careful calculation and evaluation indicated that, within an acceptable error limit of 5%, RO($n > 1$) model can be used to describe the degradation process of most selected fibers well. The other kinetic parameters used include activation energy range of 160–170 kJ/mol; parameter n in RO($n > 1$) = $(1 - \alpha)^n$ of 3–4; and ln A between 35 and 42 ln s^{-1}. Obtained predictive weight loss curves can simulate the thermal weight loss processes of natural fibers.

Because of strong dependence on accurate activation energy values of the Málek method, some discrepancies between predicted and experimental results at both very low and very high temperature ranges were observed. Moreover, some condition limitations of obtained model should be considered.

However, the model still has the practical significance in predicting fiber weight loss for polymer/natural-fiber composites.

References

1. Antal, M. J.; Varhegyi, G. Ind Eng Chem Res 1995, 34, 703.
2. Moghtaderi, B. Fire Mater 2006, 30, 1.
3. Yao, F.; Wu, Q. L.; Lei, Y.; Guo, W. H.; Xu, Y. J. Polym Degrad Stab 2008, 93, 90.
4. Malek, J. Thermochim Acta 1992, 200, 257.
5. Malek, J. Thermochim Acta 2000, 355, 239.
6. Malek, J.; Mitsuhashi, T.; Criado, J. M. J Mater Res 2001, 16, 1862.
7. Varhegyi, G.; Antal, M. J.; Jakab, E.; Szabo, P. J Anal Appl Pyrolysis 1997, 42, 73.
8. Antal, M. J.; Varhegyi, G.; Jakab, E. Ind Eng Chem Res 1998, 37, 1267.
9. Brown, M. E.; Maciejewski, M.; Vyazovkin, S.; Nomen, R.; Sempere, J.; Burnham, A.; Opfermann, J.; Strey, R.; Anderson, H. L.; Kemmler, A.; Keuleers, R.; Janssens, J.; Desseyn, H. O.; Li, C. R.; Tang, T. B.; Roduit, B.; Malek, J.; Mitsuhashi, T. Thermochim Acta 2000, 355, 125.
10. Maciejewski, M. Thermochim Acta 2000, 355, 145.
11. Varhegyi, G.; Antal, M. J.; Szekely, T.; Szabo, P. Energy Fuels 1989, 3, 329.
12. Vyazovkin, S. Thermochim Acta 1992, 211, 181.
13. Koga, N. Thermochim Acta 1994, 244, 1.
14. Vyazovkin, S.; Wight, C. A. Int Rev Phys Chem 1998, 17, 407.
15. Perez-Maqueda, L. A.; Criado, J. M.; Sanchez-Jimenez, P. E. J Phys Chem A 2006, 110, 12456.
16. Di Blasi, C. AIChE J 2002, 48, 2386.
17. Capart, R.; Khezami, L.; Burnham, A. K. Thermochim Acta 2004, 417, 79.
18. Di Blasi, C. Prog Energy Combust Sci 2008, 34, 47.
19. Koga, N.; Criado, J. M. Int J Chem Kinet 1998, 30, 737.
20. Koga, N.; Criado, J. M. J Am Ceram Soc 1998, 81, 2901.
21. Montserrat, S.; Malek, J.; Colomer, P. Thermochim Acta 1998, 313, 83.
22. Montserrat, S.; Malek, J.; Colomer, P. Thermochim Acta 1999, 336, 65.
23. Luangkiattikhun, P.; Tangsathitkulchai, C.; Tangsathitkulchai, M. Bioresour Technol 2008, 99, 986.